Acta Geologica Sinica (English Edition), 2019, 93(1): 241–243

Research Advances

New Discovery of Telluride and Bi-Sulfosalt in the Dahu Quartz Vein-Style Au-Mo Deposit, Xiaoqinling Region, China

YIN Chao[1, 2], LIU Jiajun[1, 2, *], ZHAI Degao[1, 2] and GUO Yuncheng[1, 2]

[1] *State Key Laboratory of Geological Processes and Mineral Resources, China University of Geosciences, Beijing 100083, China*
[2] *School of Earth Sciences and Resources, China University of Geosciences, Beijing 100083, China*

Citation: Yin et al., 2019. New Discovery of Telluride and Bi-Sulfosalt in the Dahu Quartz Vein-Style Au-Mo Deposit, Xiaoqinling Region, China *Acta Geologica Sinica* (English Edition), 93(1): 241–243. DOI: 10.1111/1755-6724.13659

Objective

The Dahu quartz vein-style Au-Mo deposit is an important deposit in the Xiaoqingling region, which contains a total reserves of 38 tons of Au at an average grade of 6.8 g/t and 100, 000 tons of Mo at an average grade of 0.24%. It is hosted in the highly metamorphic gneiss of the Archaeozoic Taihua group, and the ore-bearing quartz veins are controlled by several small to medium size E–W-striking faults, i.e., F1, F8, F7, F35, F5, and F6 from north to south (Jian et al., 2015).

The Dahu Au-Mo deposit is characterized by the common enrichment of native gold, molybdenite, telluride and Bi-sulfosalt. This work reported the new discovery of telluride and Bi-sulfosalts in this deposit, and discussed its ore genesis through systematic microscopic observation, electron probe microanalysis (Hereinafter referred to as EPMA) and thermodynamic study of mineral associations.

Methods

The samples of telluride and Bi-sulfosalt were extracted from different underground levels of ore-bearing quartz veins and wall rocks, controlled by the fault zones of F5, F7 and F35 at the Dahu Au-Mo deposit, with elevations ranging from 260 to 895 m.

Polished sections were examined by a reflecting microscope, and their minerals were analyzed by EPMA in the experimental centre of China University of Geosciences, Beijing. The EPMA instrument, equipped with wave and energy dispersive and back-scattered detector, is the SHIMADZU EPMA-1600 with an accelerating voltage set at 15 kV, current 1×10^{7} A, counting times of 20 s, and electron beam spot diameter of 1 μm. Standards and radiations used were as follows: Au metal (Mα), Ag metal (Lα), Bi_2Te_3 (Te-Lα), Bi_2S_3 (Bi-Lα), $CuFeS_2$ (Cu-Kα), PbS (Pb-Mα, S-Kα) and Bi_2Se_3 (Se-Lα). The dealing of the analysis data adopts ZAF-amendments.

Results

Ten telluride and Bi-sulfosalt minerals from the Dahu Au-Mo deposit are identified by systematic optical microscope observation and EPMA. Tellurides are mainly composed by altaite, tellurobismuthite, tetradymite and to a lesser extent by calaverite, petzite, and hessite. Meanwhile, a certain amount of Bi-sulfosalt minerals are found, including aikinite, lindstromite, saddlebackite and hammarite. Telluride and Bi-sulfosalt all have a genetic relationship with native gold. Representative EPMA data for these minerals are presented in Appendix 1. In addition, thermodynamic modeling is used to constrain the physicochemical conditions during ore formation (Fig. 1). These ore mineral associations identified at the Dahu deposit are very similar to other magmatic-hydrothermal Au-Te deposits, i.e., the Kochbulak and Kariagach deposits in Uzbekistan (Plotinskaya et al., 2006), the Perama Hill deposit in Greece (Voudouris et al., 2011). These new evidences for telluride and Bi-sulfosalt mineral associations and phsicochemical conditions support a magmatic-hydrothermal origin model for the Dahu Au-Mo deposit.

Conclusions

(1) The Dahu Au-Mo deposit is rich in tellurides as well as significant amounts of Bi-sulfosalt. Telluride mineralization is composed of altaite, tellurobismuthite, tetradymite, and to a lesser extent of petzite, calaverite, hessite. The present Bi-sulfosalts are aikinite, lindstromite, saddlebackite and hammarit. They all have a genetic relationship with native gold.

(2) Thermodynamic calculations and simulation results show that tellurides substantially precipitated in the Dahu Au-Mo deposit under physicochemical conditions of T=240°C, $\log f Te_2$=−13.3–−8.1, $\log f S_2$=−14.6–−9.

(3) The Au-Ag-Te-Mo-Bi metallogenic element assemblages of the Dahu Au-Mo deposit were mostly derived from a magmatic-hydrothermal system.

Acknowledgments

This work was financially supported by the National Natural Science Foundation of China (grants No. 41573036 and 41730426) and Fundamental Research

* Corresponding author. E-mail: liujiajun@cugb.edu.cn

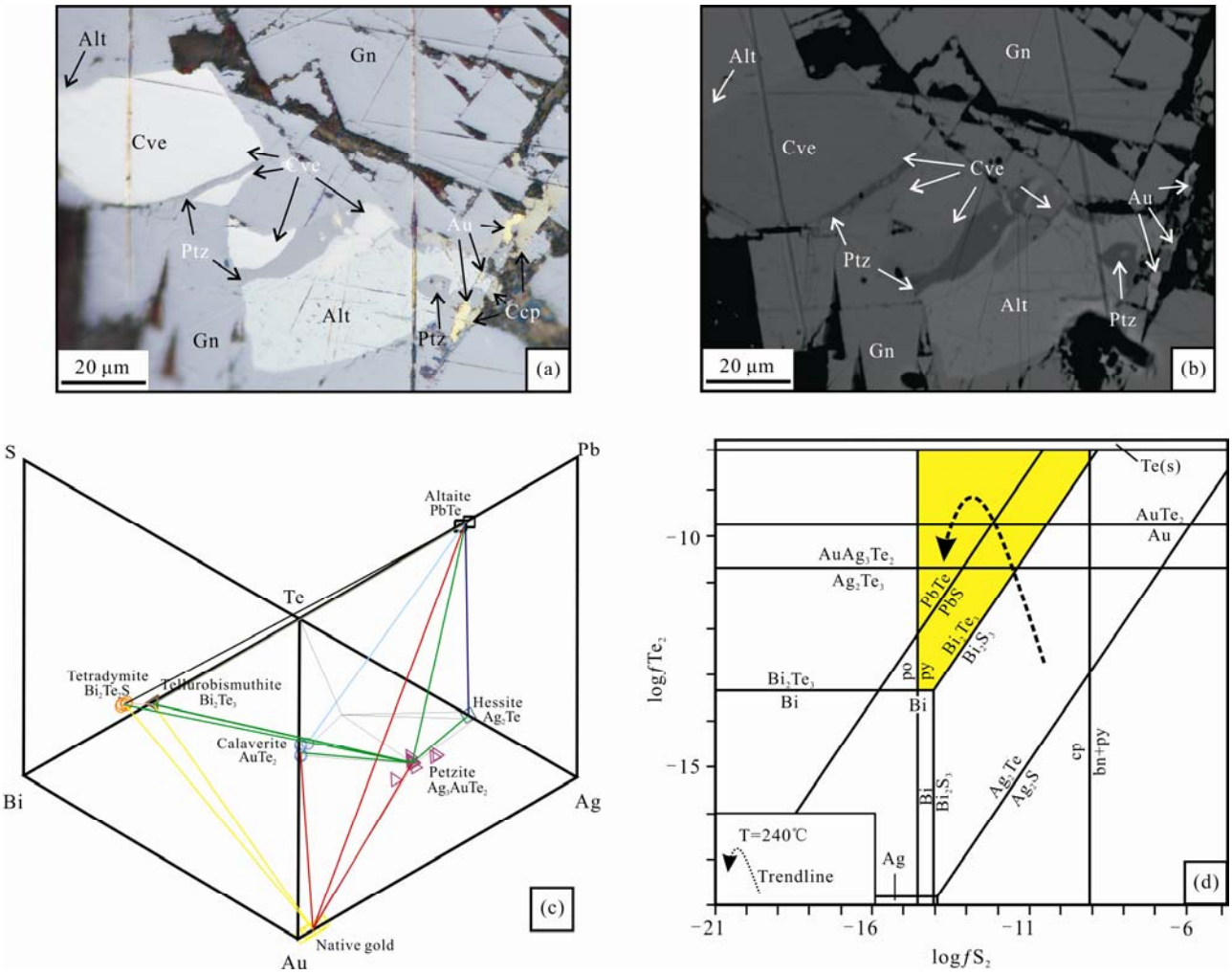

Fig. 1. (a), Representative photomicrographs of telluride samples showing native gold coexist with altaite, calaverite, petzite and chalcopyrite (reflected light, sample 16DH-41/F7. 295); (b), Representative BSE image of Fig. 1a; (c), Au-Ag-Te-Bi-Pb-S diagram showing the Dahu telluride and native gold assemblages; (d), logfTe_2 vs. logfS_2 diagram for phase equilibrium in the Au-Ag-Te-Bi-S system for telluride and Bi-sulfosalt stage at 240°C. The yellow field represents the stability field of telluride assemblage equilibrium at 240° C. The black solid lines represent the boundaries of calverite-natve gold, petzite-hessite, tellurobismuthite-bismuth, bismuthinite-bismuth, altaite-galena, tellurobismuthite-bismuthinite, hessite-acanthite, pyrrhotite-pyrite and chalcopyrite-bornite+pyrite, respectively, and the dashed curve line ① represents the evolution trend of telluride species. Abbreviations: po-pyrrhotite, py-pyrite, cpy-chalcopyrite, bn-bornite.

Funds for the Central Universities, China University of Geosciences (grant No. 2652017263). We are indebted to Prof. Yin Jingwu, Hao Jinhua and Kong Dexin of Electron Probe Laboratory, China University of Geosciences (Beijing) for their help with EPMA analysis.

References

Jian Wei, Lehmann Berand, Mao Jingwen, Ye Huishou, Li Zongyan, He Haijiang, Zhang Jinge, Zhang Hai and Feng Jiangwei, 2015. Mineralogy, fluid characteristics, and Re-Os age of the Late Triassic Dahu Au-Mo deposit, Xiaoqinling region, Central China: evidence for a magmatic-hydrothermal Origin. *Economic Geology*, 110: 119–145.

Plotinskaya, O.Y., Kovalenker, V.A., Seltmann, R., and Stanley, C.J., 2006. Te and Se mineralogy of the high-sulfidation Kochbulak and Kairagach epithermal gold telluride deposits (Kurama Ridge, Middle Tien Shan, Uzbekistan). *Mineralogy and Petrology*, 87: 187–207.

Voudouris, P.C., Spry, P.G., Moritz, R., Papavassiliou, C., and Falalakis, G., 2011. Mineralogy and geochemical environment of formation of the Perama Hill high-sulfidation epithermal Au-Ag-Te-Se deposit, Petrota Graben, NE Greece. *Mineralogy and Petrology*, 103: 79–100.

Appendix 1 Representative electron microprobe analyses (wt%) of tellurides and Bi-sulfosalts from the Dahu Au-Mo deposit

Mineral	1	2	3	4	5	6	7	8	9	10	11	12	13	14	15	16	17	18
Au	bd	bd	bd	bd	bd	0.05	38.46	39.01	24.88	32.82	0.57	0.14	0.01	0.13	0.15	bd	0.06	bd
Ag	bd	bd	0.31	0.25	0.48	0.32	0.79	0.75	40.27	34.53	55.44	bd	bd	bd	bd	0.06	bd	bd
Te	37.00	36.45	47.13	46.92	39.75	41.07	58.78	59.01	35.78	32.68	44.00	0.09	0.21	0.07	bd	19.17	0.01	bd
S	4.51	4.35	bd	bd	bd	bd	0.04	0.02	0.03	0.05	0.09	17.60	17.77	18.96	16.78	9.25	17.70	17.74
Bi	57.13	57.99	51.97	51.37	0.43	0.48	0.99	bd	bd	bd	bd	36.68	37.14	54.47	58.66	32.28	45.18	48.75
Cu	0.06	0.01	0.02	0.02	0.07	bd	0.08	0.08	0.03	0.11	0.02	9.95	9.55	5.17	5.21	0.09	9.81	8.85
Pb	bd	0.07	bd	bd	57.95	58.19	bd	bd	0.42	0.21	0.08	35.46	34.46	20.26	18.91	39.80	26.31	23.57
Se	0.10	0.07	0.21	0.06	bd	0.03	0.04	0.04	bd	0.01	0.03	0.06	0.12	0.01	0.04	0.07	0.01	0.01
Total	98.80	98.94	99.63	98.63	98.68	100.14	99.17	98.90	101.40	100.41	100.22	99.99	99.27	99.07	99.76	100.73	99.08	98.93
Atoms	5	5	5	5	2	2	3	3	6	6	3	6	6	28	28	9	17	17
Au	-	-	-	-	-	0.00	0.87	0.89	0.97	1.34	0.01	0.00	-	0.02	0.02	-	0.01	-
Ag	-	-	0.02	0.02	0.01	0.01	0.03	0.03	2.86	2.57	1.78	-	-	-	-	0.01	-	-
Te	2.05	2.04	2.96	2.98	1.04	1.06	2.06	2.07	2.15	2.06	1.20	0.00	0.01	0.01	-	1.72	0.00	-
S	1.00	0.97	-	-	-	-	0.01	0.00	0.01	0.01	0.01	3.12	3.16	16.04	14.97	3.29	8.63	8.95
Bi	1.94	1.98	1.99	1.99	0.01	0.01	0.02	-	-	-	-	1.00	1.01	7.07	8.03	1.76	3.31	2.83
Cu	0.01	0.00	0.00	0.00	0.00	-	0.01	0.01	0.00	0.01	0.00	0.89	0.86	2.21	2.35	0.02	2.48	2.52
Pb	-	0.00	-	-	0.93	0.92	-	-	0.02	0.01	0.00	0.97	0.95	2.65	2.61	2.19	2.55	2.67
Se	0.01	0.01	0.02	0.01	-	0.00	0.00	0.00	-	0.00	0.00	0.00	0.01	0.00	0.02	0.01	0.03	0.02

Note: 1–2, Tetradymite; 3–4, Tellurobismuthite; 5–6, Altaite; 7–8, Calaverite; 9–10, Petzite; 11, Hessite; 12–13, Aikinite; 14–15, Lindstromite; 16, Saddlebackite; 17–18, Hammarite. Abbreviation: bd, Below detection limit (0.01%).